Supplementary figures

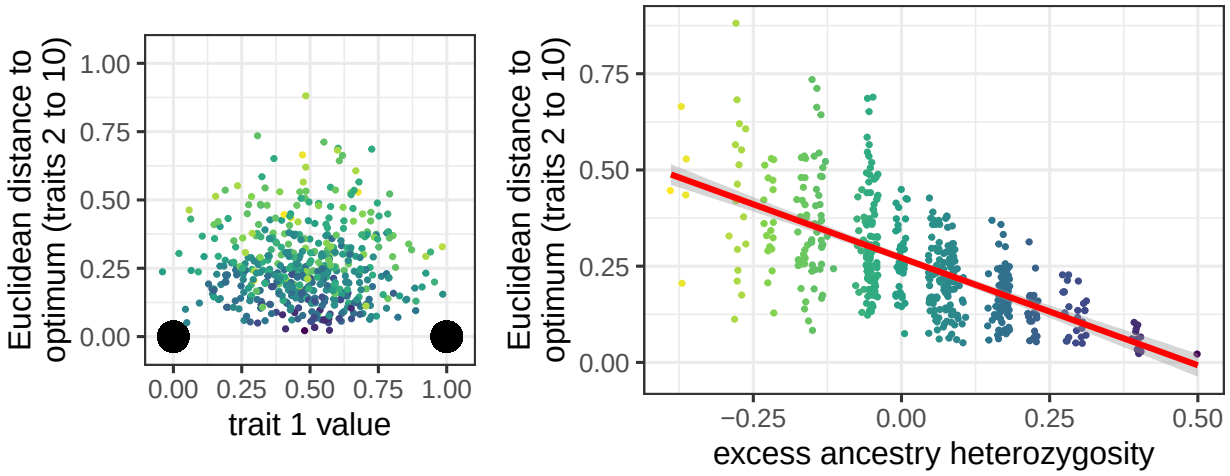

Figure S1: **Simulation model illustrating the incompatibility–heterozygosity relationship.** The model is as in Fig. 1 in the main text except there are ten traits instead of two and the optimum of the adapting population is '0' for traits 2–9. Plots and model are inspired by Fig. 1 in Barton (2001). Both panels depict results from a representative simulation run of adaptive divergence and hybridization between two populations. Coloured points are individual hybrids, with darker colours indicating higher heterozygosity. Panel (A) depicts the distribution of 500 F_2 hybrid phenotypes where the x-axis depicts the value of the selected trait, and the y-axis depicts the Euclidean distance from the optimum for traits 2–9 (i.e., $y = \sqrt{\sum_{i=2}^{10} z_i^2}$). Large black points are the two parent phenotypes. Panel (B) depicts the relationship between excess ancestry heterozygosity and the maladaptive distance from the optimum for individual hybrids (Thompson et al., 2021). Points are slightly jittered horizontally. The plot shows that this maladaptive trait expression is lower in F_2s with greater excess ancestry heterozygosity. Heterozygosity values are fairly discrete because a small number of loci underlie adaptation in the plotted simulation run.

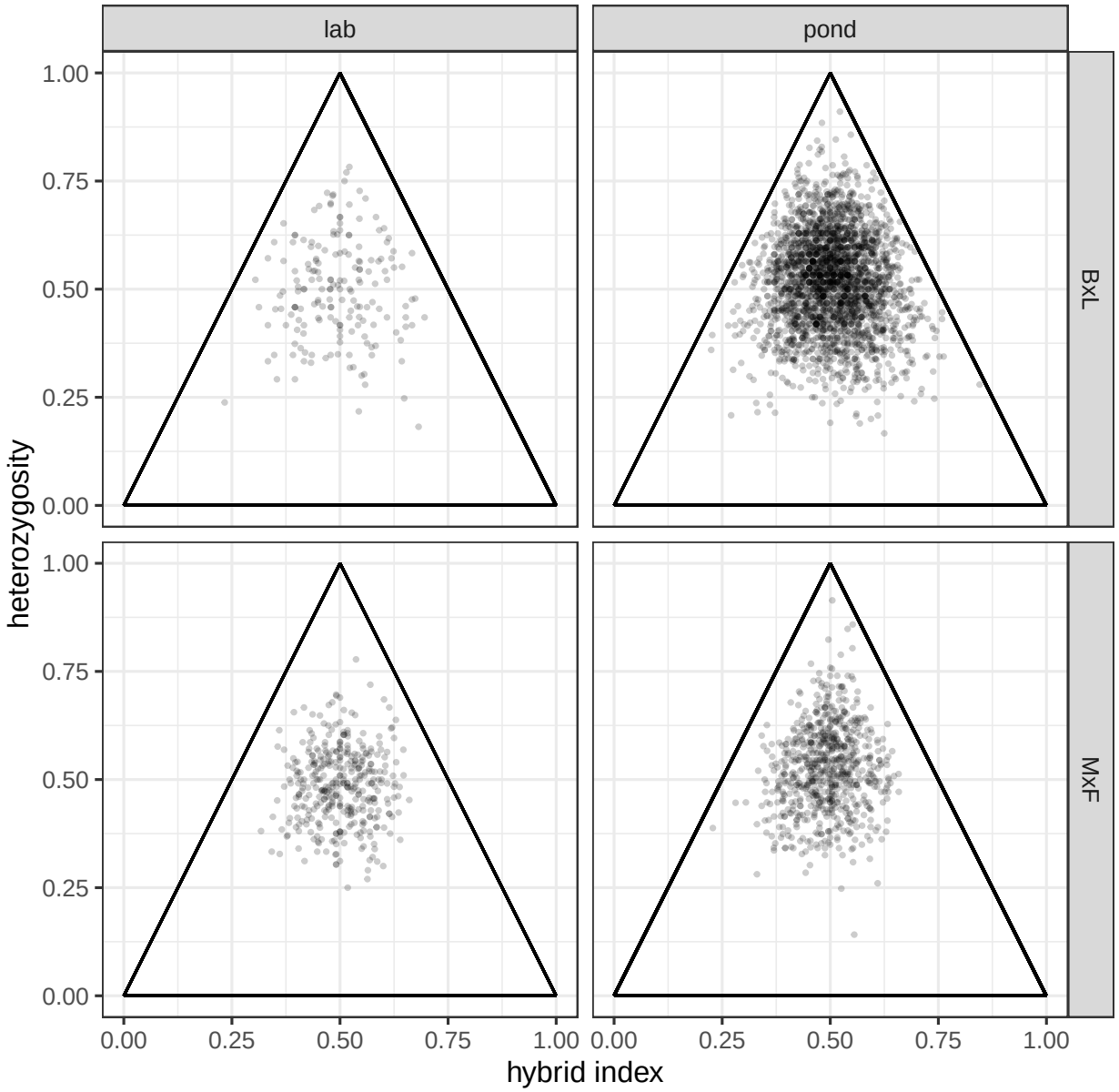

Figure S2: **de Finetti ternary diagrams for genotyped *individuals*.** Each point represents an individual hybrid and shows each individual's hybrid index (frequency of benthic or marine alleles in its genome) and its mean heterozygosity. Hybrid index and heterozygosity are used because many loci are being considered simultaneously. These graphs are not used for analysis, but rather are shown to allow readers to visualise the structure of the raw data that underlies our analysis. Specifically, the shapes of the distributions of heterozygosity and hybrid index values are similar between environments and crosses—the means are just subtly different.

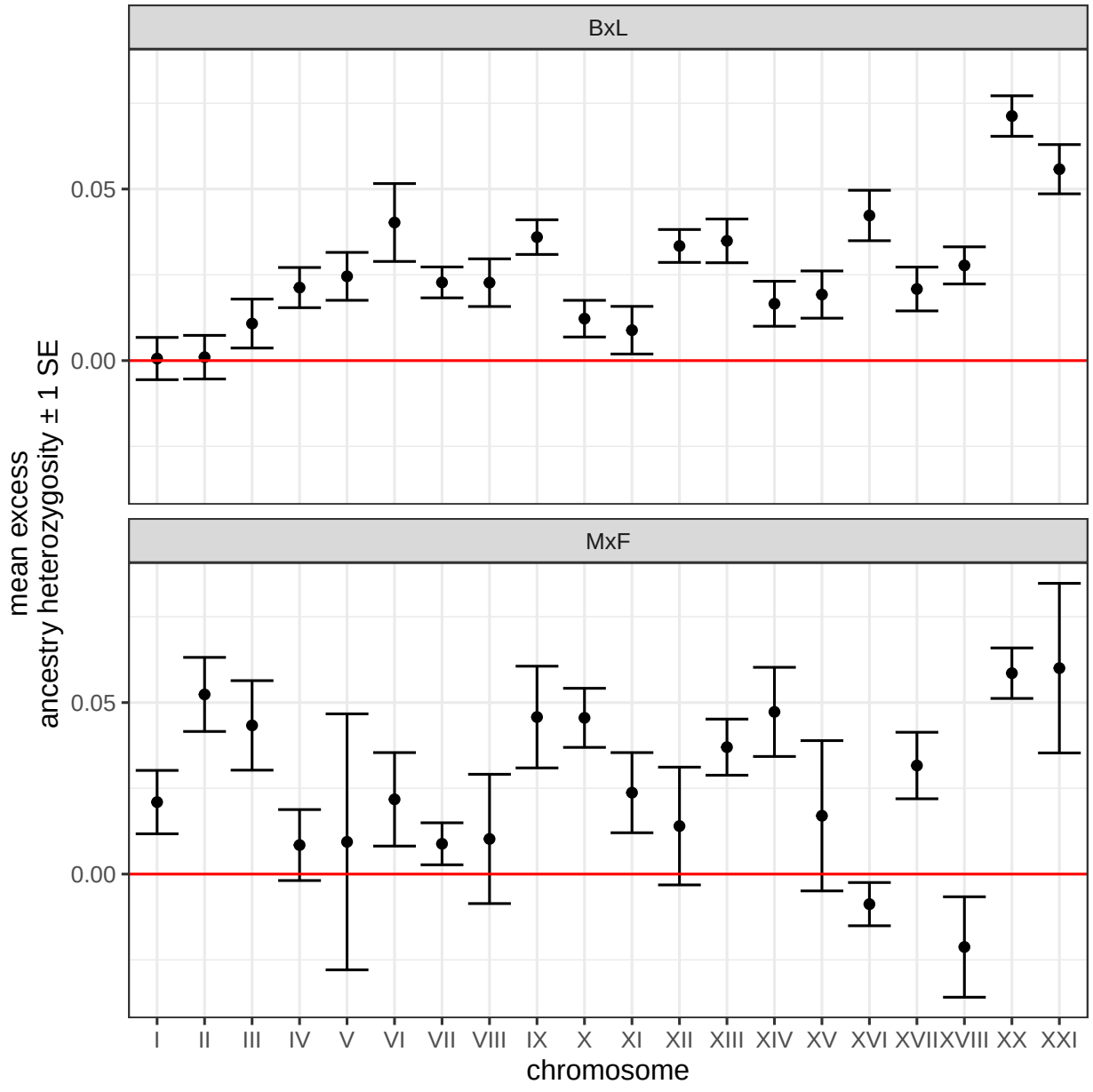

Figure S3: **Mean excess ancestry heterozygosity across chromosomes.** Each point is the average excess ancestry heterozygosity for all loci on a given chromosome (raw values; not residuals from a statistical model). Linkage group XIX contains the sex determining region and is not shown. Error bars are 1SE.

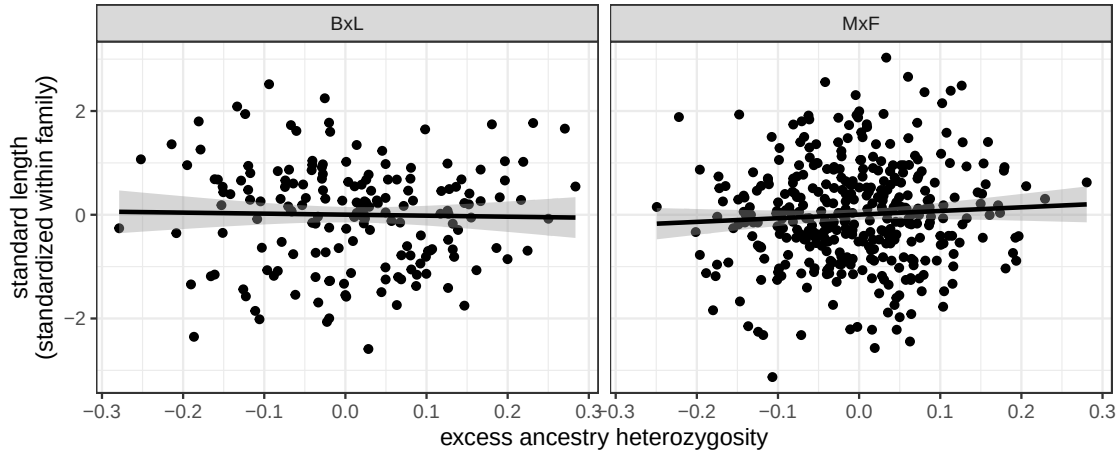

Figure S4: **No relationship between individual mean heterozygosity and growth (standard length) in the aquarium-raised biparental benthic-limnetic F_2 hybrids.** Results are residuals from `visreg` (Breheny and Burchett, 2017). Each point is an individual F_2 hybrid. Standard length is standardized within family (one family each for Paxton and Priest lakes for B×L and four families for M×F. The interaction between lake-of-origin mean heterozygosity was non-significant so we plot the main effect across both lakes-of-origin (Paxton and Priest). Mean heterozygosity was not significantly associated with standard length for either cross (B×L—$\hat{\beta}$ = $-0.05\pm$ 0.67 [SE], $F_{1,174}$ = 0.0075, P = 0.93; M×F—$\hat{\beta}$ = 0.65 $\pm$ 0.59 [SE], $F_{1,372}$ = 1.24, P = 0.26). Analyses considering body depth (either individually or in a combined metric of 'overall size') give the same qualitative result (not shown).

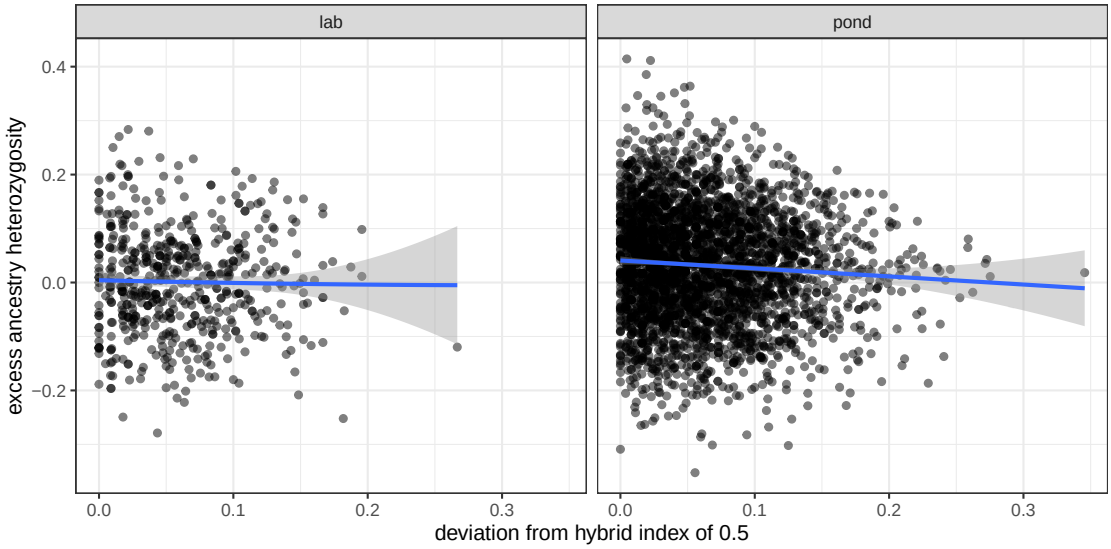

Figure S5: **The benefit of excess heterozygosity declines with deviations from a hybrid index of 0.5 in ponds but not in the lab.** Each point is an individual recombinant hybrid and data are pooled across cross types. Excess ancestry heterozygosity declines as the hybrid index of pond-raised individuals deviates from 0.5 (Spearman's $\rho = -0.059$; $P = 0.0006$), whereas there is no relationship in the lab ($\rho = -0.012$; $P = 0.77$). Bootstrap tests indicate that these two correlations are statistically indistinguishable, so we consider this analysis to be interesting and consistent with our hypothesis, but not conclusive.

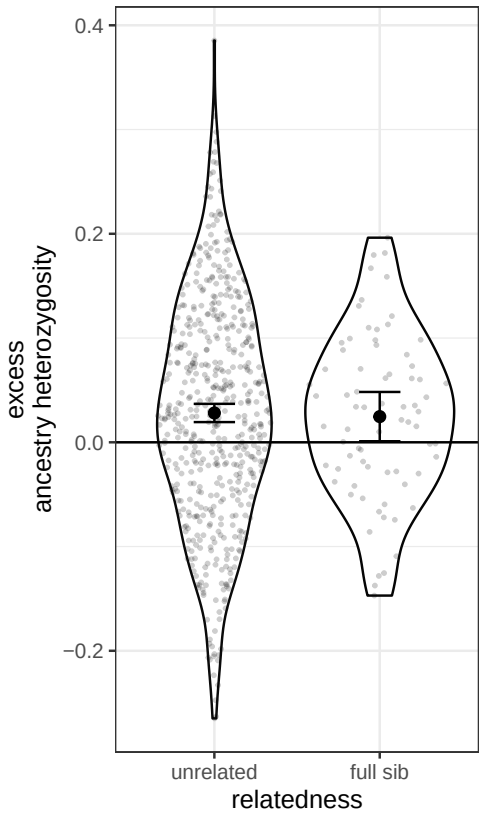

Figure S6: **Comparing selection on ancestry heterozygosity between individuals of different relatedness.** There is no difference in mean excess ancestry heterozygosity between F_2 hybrids whose parents were unrelated and those whose parents were full siblings. Data from Arnegard et al. (2014).

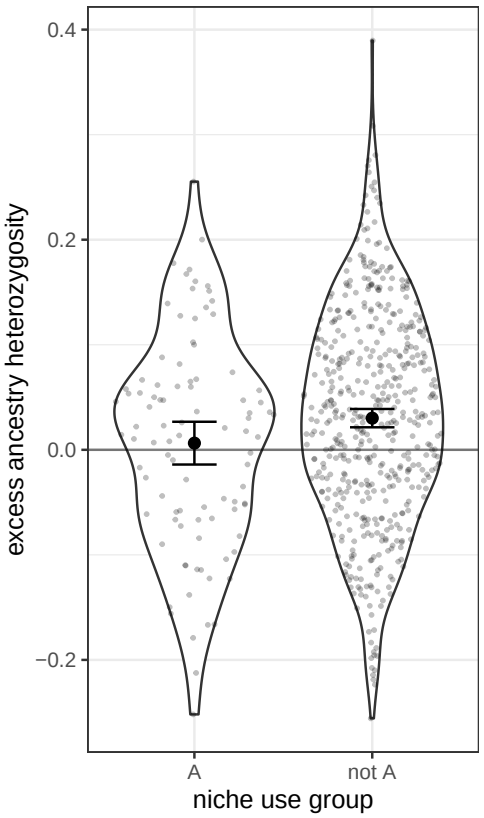

Figure S7: **Fish assigned *a priori* as 'phenotypically mismatched' ('A' group) have lower excess ancestry heterozygosity than non-mismatched fish.** Assignments are from Arnegard et al. (2014) and methods are described therein. Each point is an individual F_2 hybrid. This result implies that phenotypically mismatched individuals have lower excess ancestry heterozygosity than non-mismatched individuals.

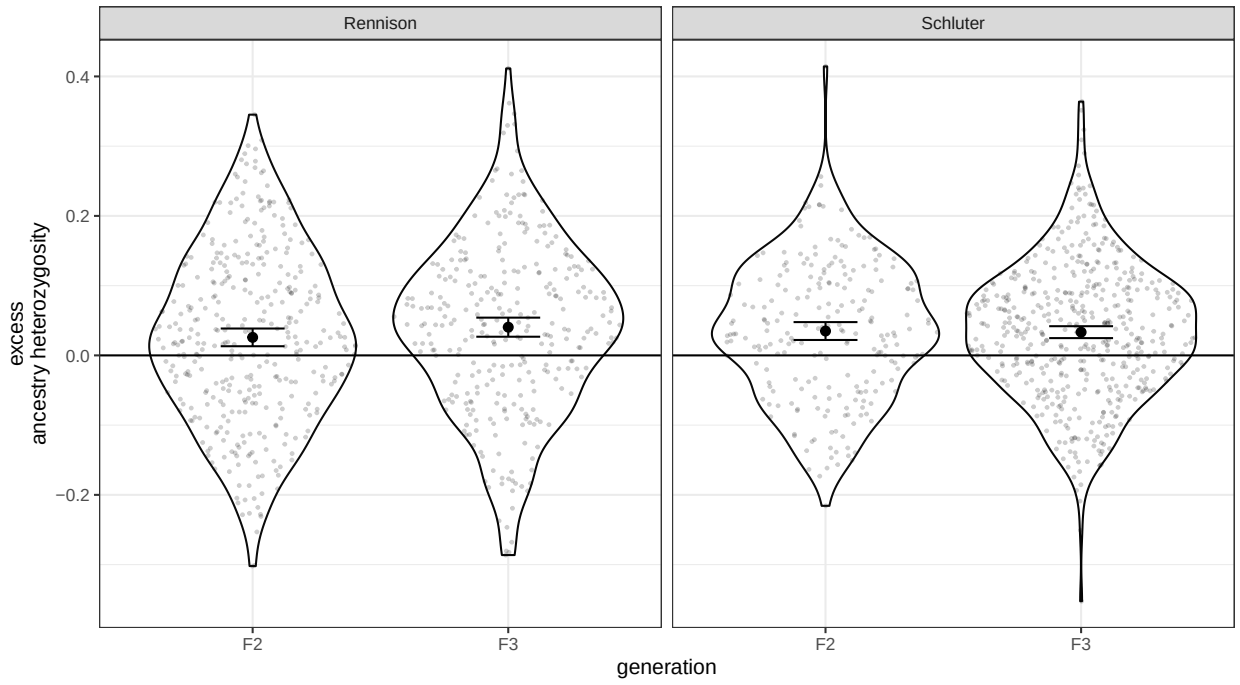

Figure S8: **Excess ancestry heterozygosity does not differ between F_2 and F_3 hybrids.** The plots show individual excess ancestry heterozygosity from the two studies that genotyped both the F_2 and F_3 generations (Schluter et al., 2021; Rennison et al., 2019). The means (black dots, ± 95 % CI) do not differ between generations in either study (Rennison group difference = 0.014 ±0.0095 [SE], $F_{1,667}$ = 2.35, P = 0.13; Schluter group difference = 0.0016 ±0.0078 [SE], $F_{1,721}$ = 0.042, P = 0.84).

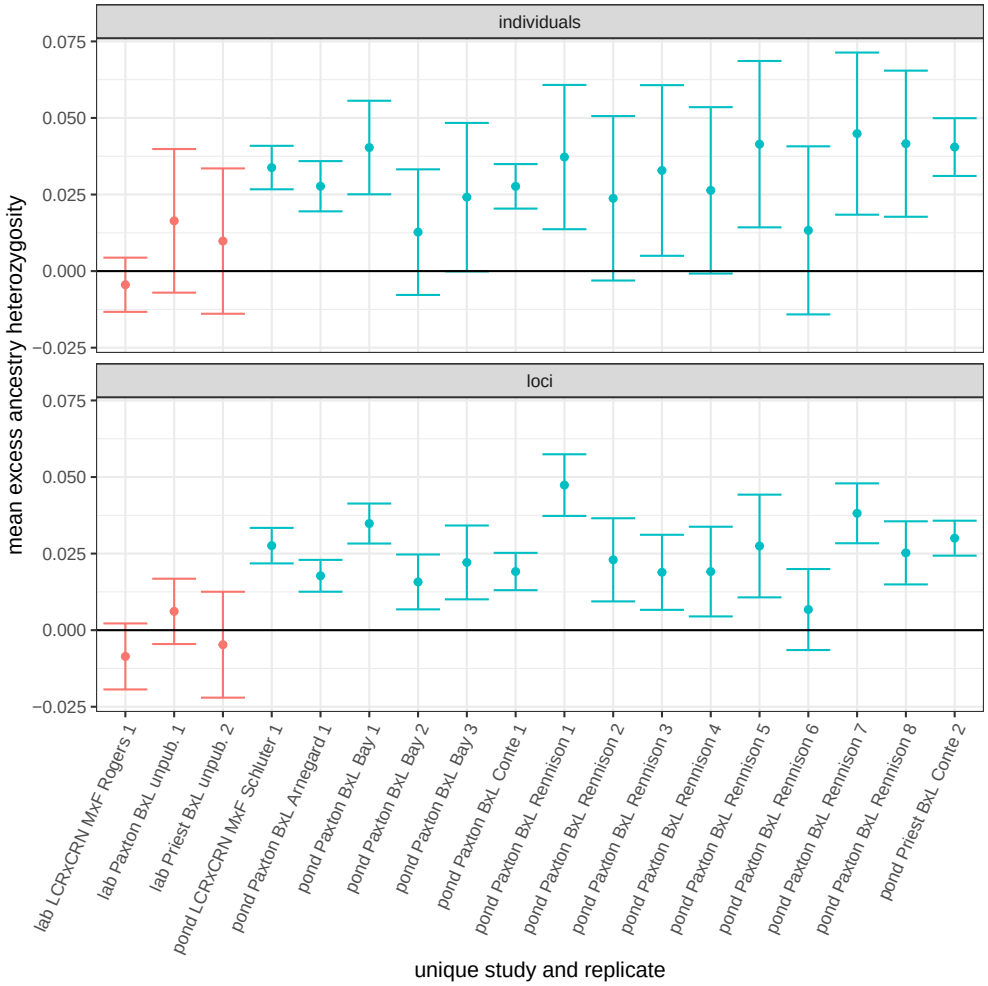

Figure S9: **Estimates of mean (± 95% CI) excess ancestry heterozygosity for individuals and loci across 'replicates'.** We consider a replicate to be a unique bi-parental F_0 cross for aquarium studies, and a unique pond for pond studies. Mean excess ancestry heterozygosity is shown for each such replicate for both individuals (upper) and loci (lower). In each panel the horizontal line indicates no excess ancestry heterozygosity. Red points are 'lab' replicates, and blue points are 'pond' replicates.

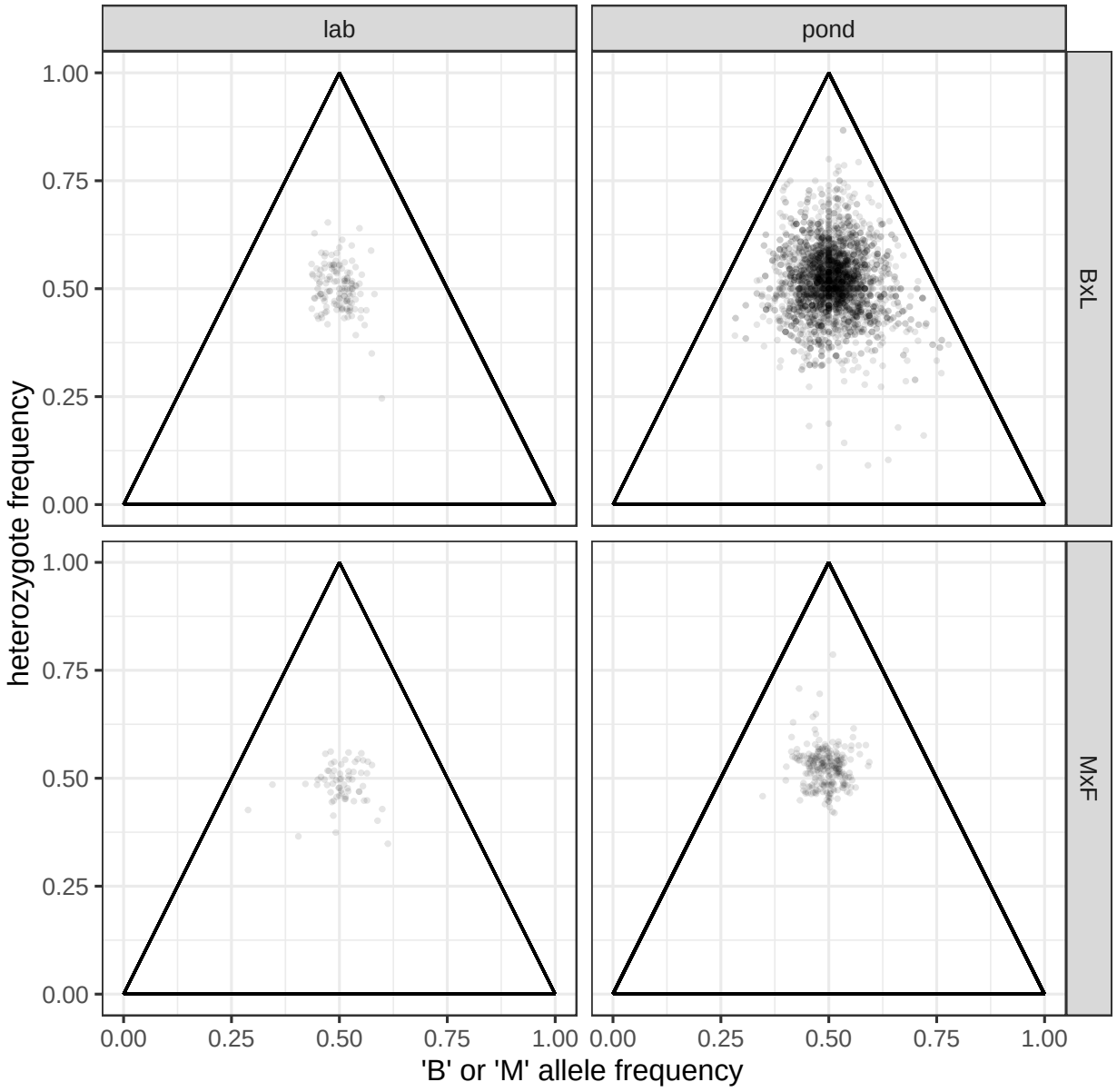

Figure S10: **de Finetti ternary diagrams for genotyped *loci*.** Each point represents genotyped locus within a given study (i.e., line in Table 1 in the main text) and shows the frequency of either benthic or marine alleles on the *x*-axis and its heterozygosity on the *y*-axis. These graphs are not used for analysis, but rather are shown to allow readers to visualise the structure of the raw data that underlies our analysis. Specifically, the shapes of the distributions of heterozygosity and hybrid index values are similar between environments and crosses—the means are just subtly different.

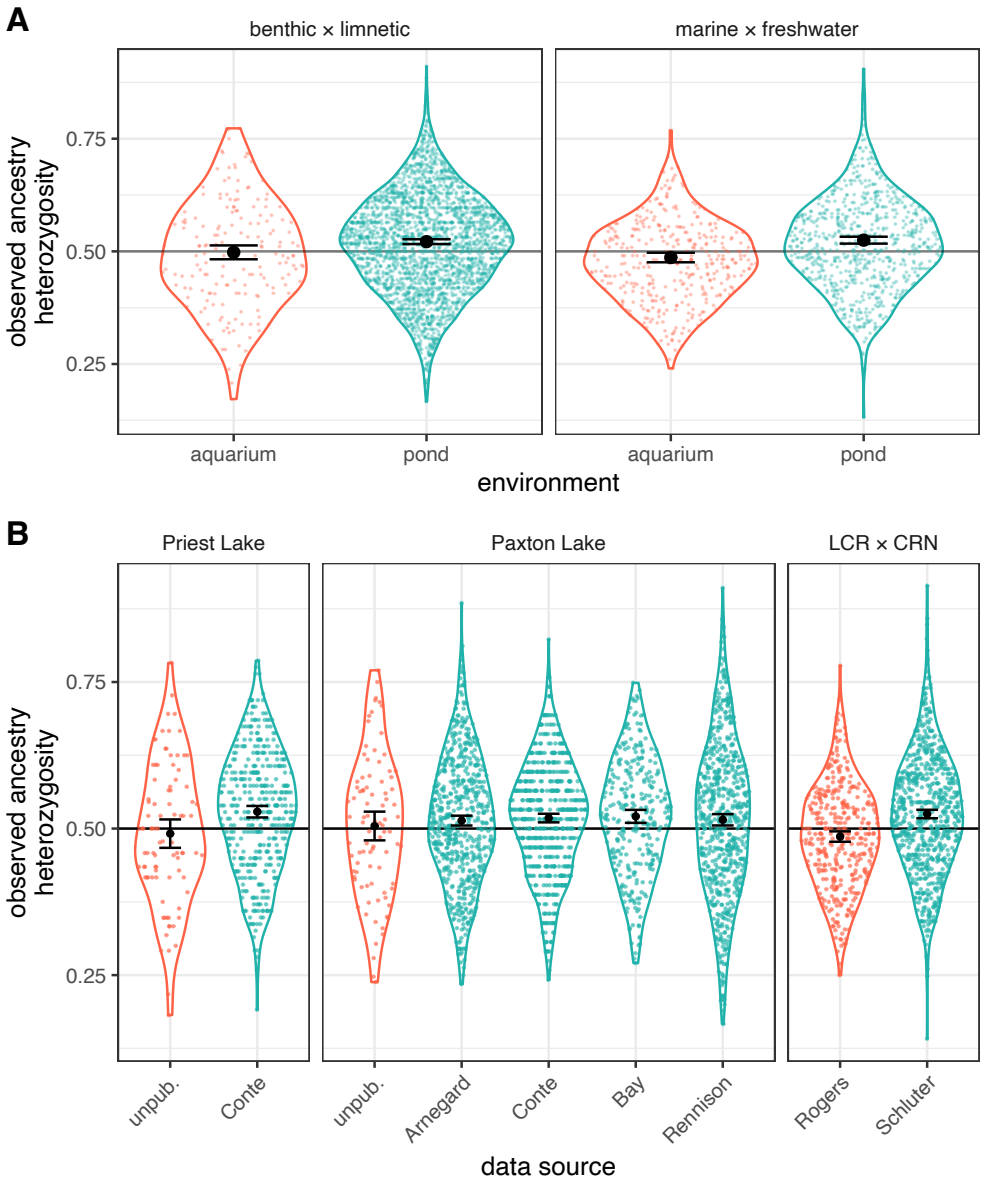

Figure S11: **Main analysis with *observed* ancestry heterozygosity rather than *excess* ancestry heterozygosity as the response.** For full details, see caption of Fig. 2 in the main text. Qualitative conclusions of statistical models are identical to those of the main analysis (see archived R script).

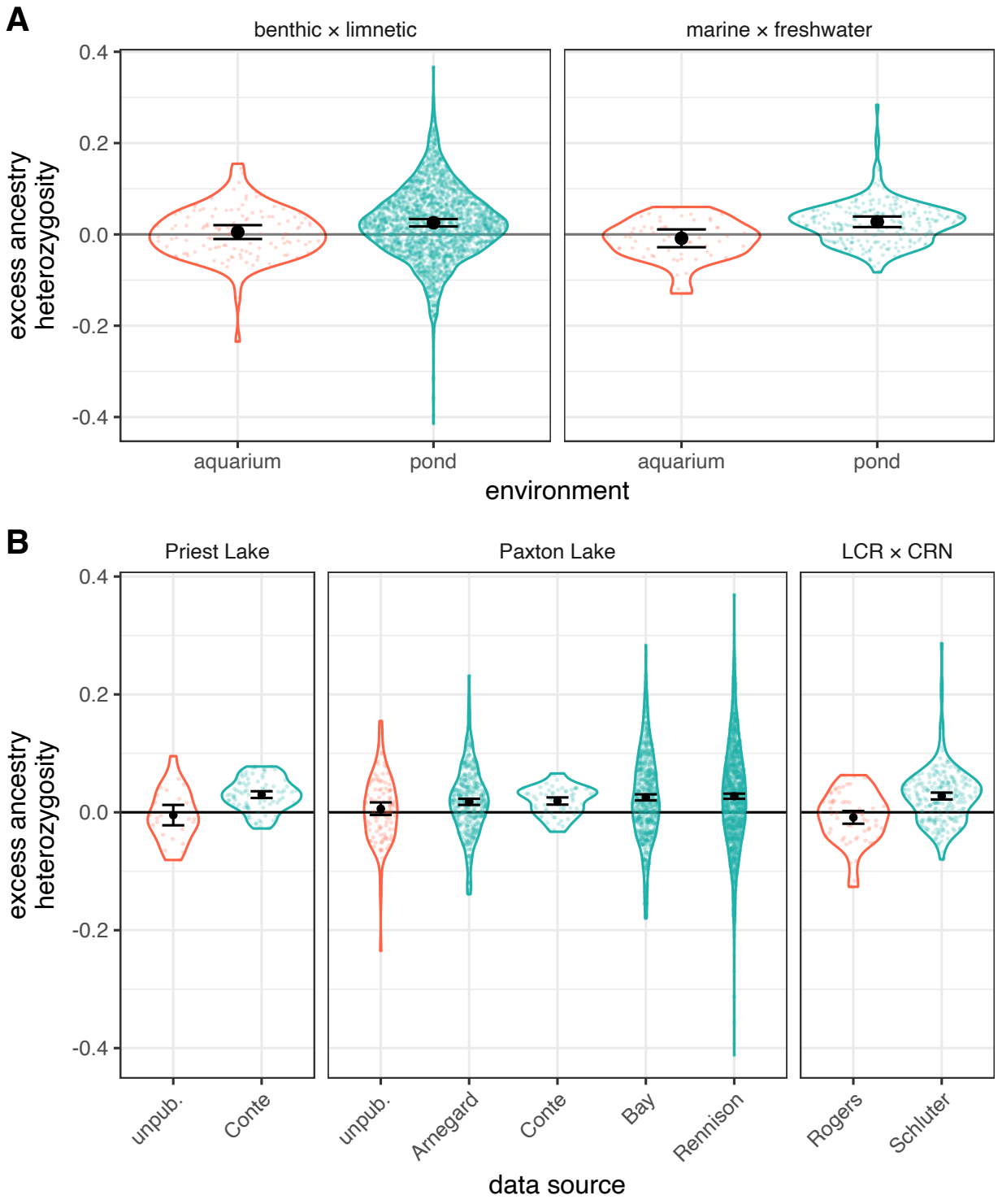

Figure S12: **Test of main hypothesis with loci instead of individuals.** Figure is as in Fig. 2 in the main text (and Fig. S11) and qualitative conclusions of statistical models are identical to those of the main analysis (see archived R script).